FLOW OF A HYDROMAGNETIC VISCOUS FLUID BETWEEN PARALLEL DISKS WITH SLIP

N. Khan *

Department of Mathematics
The Islamia University of Bahawalpur
Bahawalpur, Pakistan

M. Sajid

Theoretical Physics Division
The Pakistan Institute of Nuclear Science and Technology
Islamabad, Pakistan

T. Mahmood

Department of Mathematics
The Islamia University of Bahawalpur
Bahawalpur, Pakistan

ABSTRACT

The present paper is devoted to the investigation of steady MHD axi-symmetric flow between two infinite stretching disks with slip effects. Our attention lies in obtaining the similarity solutions of the governing partial differential equations. The transformed boundary value problem is solved analytically for a series solution using homotopy analysis method. The convergence of the obtained solution is established and fluid velocity and pressure are analyzed for various set of parameter values. The obtained results are valid for both moderate and large values of Reynolds number.

Keywords: Magnetohydrodynamics, Stretching disks, Slip boundary condition, Homotopy analysis method.

1. INTRODUCTION

A glance at the literature suggests that fluid flows due to stretching boundary have got enormous attractions by the researchers studying the theoretical aspects of Newtonian and non-Newtonian fluids. This is due to the fact that stretching flows have many industrial and technological applications. This includes the metal formation [1], polymer extrusion [2], drawing of plastic films [3] *etc*. The flow of a viscous fluid over a moving flat plate was analyzed theoretically by Sakiadis [4,5]. Crane [6] obtained a closed form analytic solution for the flow past a stretching surface for the first time. Crane's problem was one of the rare problems in fluid dynamics that possesses the closed form exact solution. The Crane's problem has been addressed by many researchers for viscous fluids by incorporating different aspects of flow and heat transfer. For the details readers are referred to the articles [7-12] and references therein. Fang [13] investigated the flow over a stretching disk. In another study Fang and Zhang [14] presented a solution of the axisymmetric flow between stretching disks using regular perturbation method for small values of the Reynolds number and an asymptotic solution for the large values of Reynold number. The study also includes the numerical solution for all range of Reynolds number. Gorder *et al*. [15] employed the homotopy analysis method to discuss the flow problem presented in [13].

In general the fluid flow problems are solved by implementing the no-slip boundary condition at the surface. However, when the fluid is a polymer or emulsion and the surface is sufficiently smooth this no-slip condition is no more valid. The flow over a stretching sheet with partial slip has been investigated by Wang [16] for a numerical solution. Anderson [17] presented an exact solution of the problem considered in [16]. The effects of slip on the axisymmetric flow past a stretching sheet are analyzed by Ariel [18]. Unsteady axisymmetric flow of a viscous fluid over a stretching sheet has been investigated by using homotopy analysis method by Sajid *et al*. [19]. In a recent study Sajid *et al*. [20] imposed the general slip boundary condition to discuss the stretching flow of a viscous fluid.

In the present paper we are interested in investigating the axisymmetric flow of a viscous fluid between stretching disks in the presence of an applied magnetic field with slip at the lower disk. The Navier slip boundary condition has been used to discuss the MHD flow in the low magnetic Reynolds number approximation. The detail discussion on the low magnetic Reynolds number approximation can be seen in the book by Davidson [21]. The analytic series solutions are developed using homotopy analysis method [22-34] for both moderate and large values of the Reynolds number. The paper is structured as follows: Section 2

* Corresponding author (nargiskhan49@gmail.com)

DOI : 10.1017/jmech.2015.25
Copyright © 2015 The Society of Theoretical and Applied Mechanics, R.O.C.
https://doi.org/10.1017/jmech.2015.25 Published online by Cambridge University Press

contains the mathematical formulation of the problem. The analytic solution for both moderate and large Reynolds number is presented in Section 3. Section 4 is devoted to the obtained results and their discussion. Some conclusions are presented in Section 5.

2. MATHEMATICAL FORMULATION OF THE PROBLEM

Consider a steady, axi-symmetric, laminar flow of an electrically conducting viscous fluid between two stretchable infinite disks. Disks are kept at a distance d from each other. It is assumed that both disks are linearly stretching in the radial direction. The fluid occupies the space $0 < z < d$. A constant magnetic field $\boldsymbol{B_0}$ is applied in the transverse direction to the flow. The induced magnetic field is neglected under the low magnetic Reynold number approximation. For mathematical modeling, we use cylindrical coordinate (γ, θ, z) and due to axisymmetry the azimuthal component of velocity vanishes and all quantities are independent of θ. The equations that govern the MHD axisymmetric flow of a viscous fluid are

$$\frac{1}{r}\frac{\partial}{\partial r}(ru) + \frac{\partial w}{\partial z} = 0, \tag{1}$$

$$u\frac{\partial u}{\partial r} + w\frac{\partial u}{\partial z} = -\frac{1}{\rho}\frac{\partial p}{\partial r} + \nu\left(\frac{\partial^2 u}{\partial r^2} + \frac{1}{r}\frac{\partial u}{\partial r} + \frac{\partial^2 u}{\partial z^2} - \frac{u}{r^2}\right) - \frac{\sigma B_0^2}{\rho}u, \tag{2}$$

$$u\frac{\partial w}{\partial r} + w\frac{\partial w}{\partial z} = -\frac{1}{\rho}\frac{\partial p}{\partial z} + \nu\left(\frac{\partial^2 w}{\partial r^2} + \frac{1}{r}\frac{\partial w}{\partial r} + \frac{\partial^2 w}{\partial z^2}\right). \tag{3}$$

The appropriate boundary conditions to the present flow situation are

$$u = ar + b_1\frac{\partial u}{\partial z}, \quad w = 0, \quad p = \frac{a\mu\beta r^2}{4d^2}, \quad \text{at} \quad z = 0$$

$$u = cr - b_2\frac{\partial u}{\partial z}, \quad w = 0, \quad p = 0, \quad \text{at} \quad z = d \tag{4}$$

in which u and w are velocity components in γ and z directions, p is pressure, ρ is density, ν is kinematic viscosity, σ is electrical conductivity, a and c are stretching rates and b_1 and b_2 are the slip lengths.

The modeled Eqs. (1) ~ (4) are partial differential equations. To reduce these ordinary differential equations, we use the similarity variables [15]

$$u = arF(\eta), \quad w = adH(\eta), \quad \eta = \frac{z}{d}$$

$$p = a\mu\left(P(\eta) + \frac{\beta r^2}{4d^2}\right). \tag{5}$$

In terms of new variables, the flow problem is governed by

$$F'' - \frac{\beta}{2} = R(F^2 + F'H) + MRF', \tag{6}$$

$$H' = -2F, \tag{7}$$

$$P' = 2RFH - 2F'. \tag{8}$$

$$F(0) = 1 + \lambda_1 F'(0), \qquad F(1) = \gamma - \lambda_2 F'(0),$$

$$H(0) = 0, \quad H(1) = 0, \quad P(0) = 0, \tag{9}$$

where

$$\gamma = \frac{c}{a}, \quad R = \frac{ad^2}{\nu}, \quad M = \frac{\sigma B_0^2}{\rho a}, \ \lambda_1 = \frac{b_1}{d}, \ \lambda_2 = \frac{b_2}{d}.$$

By using (7) in (6) and (8), we obtain as a nonlinear ordinary differential equation for the function H

$$H''' + \beta - RHH'' + \frac{R}{2}(H')^2 - MRH' = 0, \tag{10}$$

$$P' = H'' - RHH', \tag{11}$$

which is still subject to the boundary conditions

$$H(0) = 0, \qquad H(1) = 0,$$

$$H'(0) = -2 + \lambda_1 H''(0), \qquad H'(1) = -2\gamma - \lambda_2 H''(0). \tag{12}$$

Since β is a constant, therefore from Eq. (10), we have

$$H^{(iv)} - RHH''' - MRH'' = 0. \tag{13}$$

Equation (11) on integration given the pressure as

$$P = H' - \frac{RH^2}{2}. \tag{14}$$

From (10), we have an additional requirement for the parameter β.

$$\beta = -2R - H'''(0) - MRH'(0). \tag{15}$$

First we solve Eq. (13) subject to boundary conditions (12), then β can be evaluated through Eq. (15).

2.1 Skin Friction

The expression for shear stress τ_w on the surface of the stretching disk is defined as

$$\tau_w = \tau_{rz}|_{z=0},$$

The skin friction coefficients C_{1f} and C_{2f} at the lower and upper disks are

$$C_{1f} = \frac{\tau_w}{\frac{1}{2}\rho(\delta r)^2} = \frac{\tau_{rz}|_{z=0}}{\frac{1}{2}\rho(\delta r)^2} = 2Re^{-1}F'(0) = Re^{-1}H''(0),$$

$$C_{2f} = \frac{\tau_w}{\frac{1}{2}\rho(\delta r)^2} = \frac{\tau_{rz}|_{z=d}}{\frac{1}{2}\rho(\delta r)^2} = 2Re^{-1}F'(1) = Re^{-1}H''(1).$$

3. ANALYTIC SOLUTION BY MEANS OF HAM

We use the homotopy analysis method to solve the governing differential Eq. (10) subject to the boundary conditions given in Eq. (12).

https://doi.org/10.1017/jmech.2015.25 Published online by Cambridge University Press

3.1 HAM solutions to $H(\eta)$ for $0 < R < 10$

For the HAM solution we have assumed the polynomial base functions. Therefore, the initial guess for $H(\eta)$ is given by

$$H_0(\eta) = \frac{1}{-1+4\lambda_1-2\lambda_2}[-2(-1+\eta)\eta(-1+2\gamma\lambda_1+2\lambda_2+ x(1+\gamma+2\gamma\lambda_1+2\lambda_2))], \quad (16)$$

and the auxiliary linear differential operator is of the form

$$L[y] = \frac{d^4y}{d\eta^4}. \quad (17)$$

We define the zeroth order deformation equation as follows

$$(1-q)L[H(\eta;q) - H_0(\eta)] = q\hbar N[H(\eta;q)], \quad (18)$$

$$H(0,q) = H(1,q) = 0,$$

$$H'(0,q) = -2 + \lambda_1 H''(0,q),$$

$$H'(1,q) = -2\gamma - \lambda_2 H''(1,q), \quad (19)$$

$$N[H(\eta;q)] = \frac{\partial^4 H(\eta,q)}{\partial\eta^4} - MR\frac{\partial^2 H(\eta,q)}{\partial\eta^2} - RH(\eta,q)\frac{\partial^3 H(\eta,q)}{\partial\eta^3}, \quad (20)$$

when $q = 0$, we get the initial guess and when $q = 1$, we get the solution of the considered nonlinear problem. The mth order problem gives

$$L[H_m(\eta) - \chi_m H_{m-1}(\eta)] = \hbar R_m(\eta), \quad (21)$$

$$H_m(0) = H_m(1) = 0,$$

$$H'_m(0) = +\lambda_1 H''_m(0), \quad H'_m(1) = -\lambda_2 H''(1), \quad (22)$$

$$\chi_m = \begin{cases} 0, & m \le 1, \\ 1, & m > 0. \end{cases} \quad (23)$$

The solution of the problem is obtained iteratively for $m = 1, 2, 3, \ldots$ using mathematica.

3.2 HAM solutions to $H(\eta)$ for $10 < R$

To obtain an approximate analytic solution of the problem for large R, we first transform the problem by defining $\theta = \sqrt{R}\eta$ and $G = \sqrt{R}H(\eta)$. In these variables governing problem yield

$$G^{(iv)} - G(\theta)G'''(\theta) - MG''(\theta) = 0. \quad (24)$$

$$G(0) = G(\sqrt{R}) = 0,$$

$$G'(0) = -2 + \lambda_1\sqrt{R}G'''(0), \; G'(1) = -2\gamma - \lambda_2\sqrt{R}G'''(1). \quad (25)$$

The governing problem (24) subject to conditions (6) is solved using HAM by choosing following initial guess

$$G_0(\theta) = \frac{2(\sqrt{R}-\theta)\theta(-1+\eta+\eta\gamma+2(1+\eta)\gamma\lambda_1+2(1+\eta)\lambda_2)}{R(1+4\lambda_1-2\lambda_2)}. \quad (26)$$

The remaining procedure for obtaining the series solution is same as explained in previous subsection.

4. THE CONVERGENCE OF THE SOLUTION

The derived series solution to the problem contains non-zero auxiliary parameter $\hbar$. This parameter can adjust and control the convergence of the series solution. The proper values of $\hbar$ can be determined by mean of the so-called $\hbar$-curves. Figure 1(a) shows the variation of $H''(0)$ with $\hbar$ using three different order of HAM approximation for $R = 5$ and similar results for $G''(0)$ are presented in Fig. 1(b) when $R = 16$. These figures reveal that convergent results can be obtained by choosing a value for $\hbar$ in the range [–0.9, –0.1] and [–0.35, 0] respecitvely. According to Liao [31], optimal values of auxiliary parameter give better convergence, we find that the optimal value of $\hbar$ as $\hbar = -0.5$ and $\hbar = -0.27$ for small and large Reynold number respectively. Hence residual error are plotted in Fig. (2). Furthermore, the convergence of series solution is checked and shown in Table 1.

5. ANALYTICAL RESULTS AND DISCUSSION

The governing boundary value problems for both moderate and large Reynolds number are solved using the homotopy analysis method in the previous section. To see the influence of stretching ratio γ, Hartmann number M, slip parameters λ_1 and λ_2 and Reynolds number R on the velocity components in r and z directions and pressure distribution, Figs. 3 ~ 8 have been displayed. Figure 3 shows the effect of stretching ratio γ on the velocity and pressure profiles. Figure 3(a) depicts that z component of velocity is an increasing function of γ when the lower plate is stretching with a great velocity as compared with the upper plate. Qualitatively, similar results are observed in the case of large Reynolds number and plotted in Fig. 3(b). To see the impact of stretching ratio on the velocity component u we have drawn Figs. 3(c) and 3(d) respectively for moderate and large Reynolds number. It is evident from these figures that u is an increasing function of γ up to a certain height of the channel and then the velocity start decreasing with an increase in the stretching ratio. This fact is due to the difference in stretching velocities of the walls. The pressure is also increases for large values of the stretching ratio up to a certain height of the channel and then the pressure start decreasing elucidated through Figs. 3(e) and 3(f).

Table 1 Convergence of HAM solution when $\gamma = 0.25$, $M = 1$ and $\lambda_1 = 2$, $\lambda_2 = 2$.

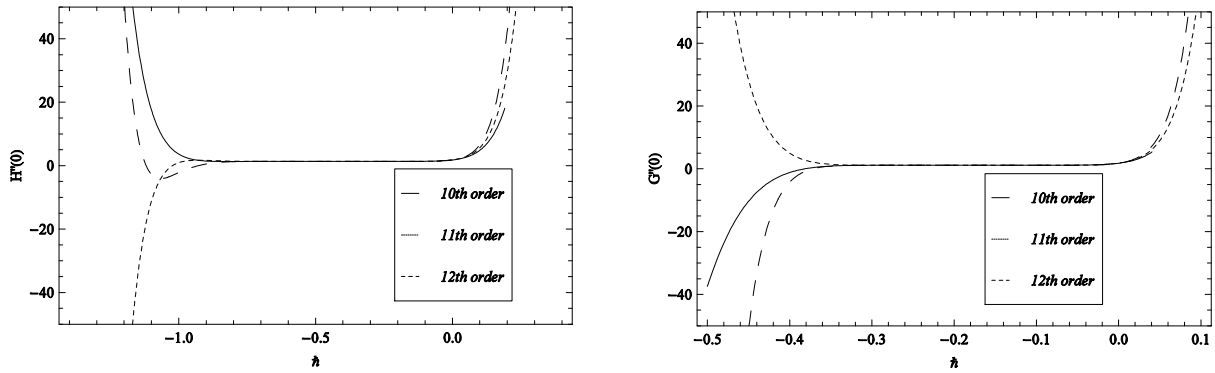
Order of Approximation	$H''(0)$	$G''(0)$
1	1.29107	0.92057
2	1.36032	1.24518
5	1.34740	1.14431
7	1.34739	1.15030
10	1.34741	1.14623
11	1.34741	1.14655
12	1.34741	1.14657

https://doi.org/10.1017/jmech.2015.25 Published online by Cambridge University Press

It reveals from Fig. 4(a), that the velocity component W decreases monotonically as the magnetic field strength increase while Fig. 4(b) present similar results in the case of large Reynolds number. In fact an increase in Hartmann number corresponds to increase in applied magnetic field. This increase in M results decrease in z-component of velocity. We have drawn Figs. 4(c) and 4(d), to observe the impact of Hartmann number on the γ component of velocity respectively for moderate and large Reynolds number. It is found that velocity component u is decreasing function of Hartmann number M upto a certain height of the channel and then the velocity start increasing. The similar trend is observed in the case of large Reynolds number. It is found from Figs. 4(c) ~ 4(f), the influence of Hartmann number M on pressure and velocity component u is qualitatively similar.

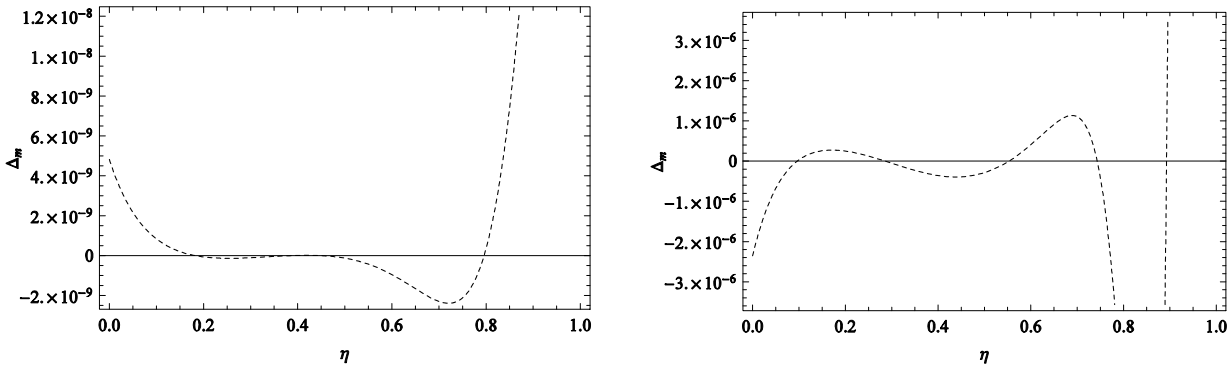
Figures 5(a) and 5(b) demonstrate the behavior of slip parameter λ_1 on z component of velocity for both moderate and large value of Reynold number. It is observed that the z component of velocity is decreasing function of slip parameter λ_1 and this behavior is qualitatively similar for both values of Reynolds number. The comparison of Figs. 4(c) ~ 4(f) with 5(c) ~ 5(f) shows that the variation of slip parameter λ_1 on velocity component u and pressure is same as that of Hartmann number. The comparison of Figs. 5 and 6 shows that the effect of slip parameter λ_2 on velocity components and pressure is opposite to that of slip parameter λ_1.

The graphs for the variation of Reynolds number on velocity components and pressure are presented in Fig. 7. It is noted that z component of velocity is decreasing function of Reynolds number R while velocity component u and pressure decreasing function of R upto a certain height of the channel and then both start increasing as Reynolds number increases. Figures 8(a) ~ 8(c) show the influence of stretching ratio γ, Hartmann number M and slip parameters λ_1 ($\lambda_2 = \lambda_1$) on pressure parameter β as a function of Reynolds number R. Figures 8(d) ~ 8(f) show the influence of Reynolds number R, Hartmann number M and slip parameters λ_1 ($\lambda_2 = \lambda_1$) on pressure parameter β as a function of stretching ratio γ. Figures 9(a) ~ 9(c) show the influence of Reynolds number R, Hartmann number M and stretching ratio γ on pressure parameter β as a function of slip parameters λ_1. Figures 9(d) ~ 9(f) show the influence of Reynolds number R, stretching ratio γ and slip parameters λ_1 ($\lambda_2 = \lambda_1$) on pressure parameter β as a function of Hartmann number M. The non-dimensional shear stress in the radial direction, namely $H''(0)$, is shown in Fig. 10 for different values of γ, M, λ_1 and λ_2 as a function of Reynolds number R. In Fig. 11, graphical results show good agreement between present analytical solution and solution obtained in [15], comparison of β for different values γ and R, and $H''(0)$ and $H''(1)$.



(a) For $R = 5$ (b) For $R = 16$

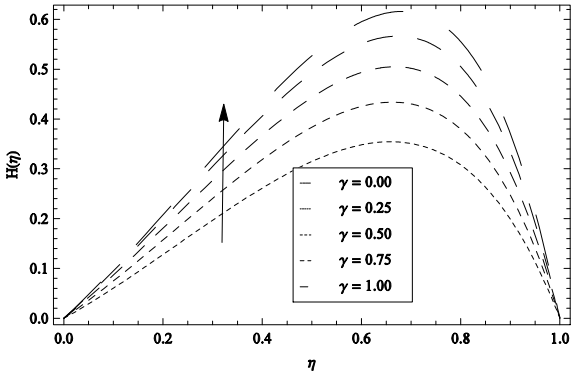
Fig. 1 $\hbar$-curves in the case of moderate Reynolds number in (a) and $\hbar$-curves in the case of large Reynolds number in (b) when $\gamma = 0.25$, $M = 1$, $\lambda_1 = 2$, and $\lambda_2 = 2$.



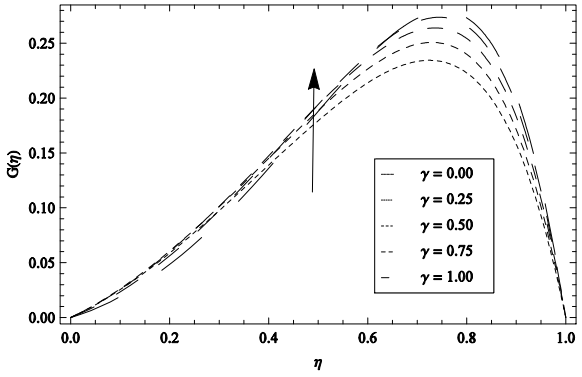
(a) For $R = 5$ (b) For $R = 16$

Fig. 2 Residual error in the case of moderate Reynolds number in (a) and residual error in the case of large Reynolds number in (b) when $\gamma = 0.25$, $M = 1$, $\lambda_1 = 2$, and $\lambda_2 = 2$.

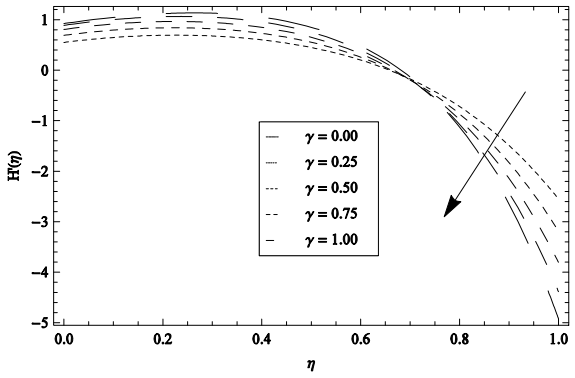
https://doi.org/10.1017/jmech.2015.25 Published online by Cambridge University Press



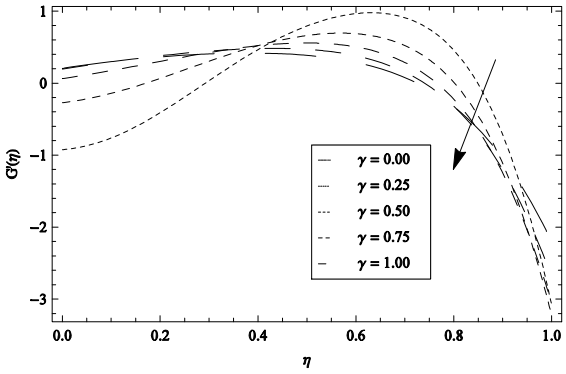
(a) For $R = 5$ and $\hbar = -0.5$



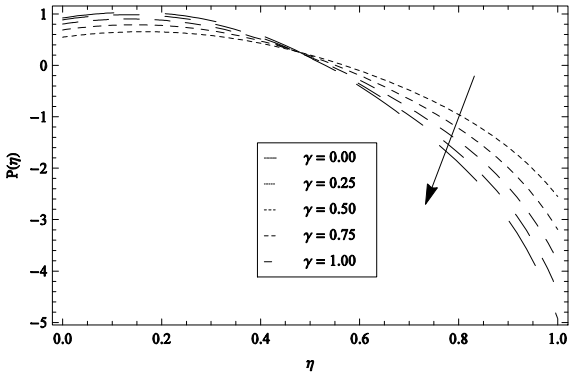
(b) For $R = 16$ and $\hbar = -0.27$



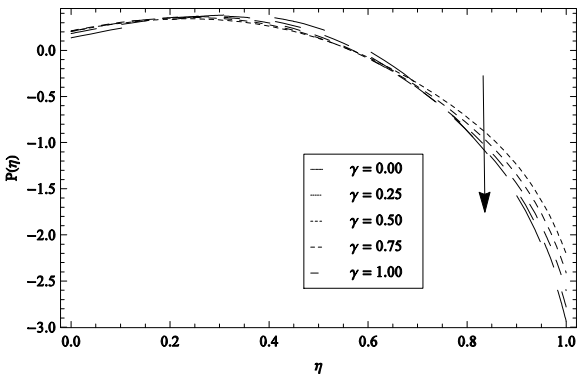
(c) For $R = 5$ and $\hbar = -0.5$



(d) For $R = 16$ and $\hbar = -0.27$



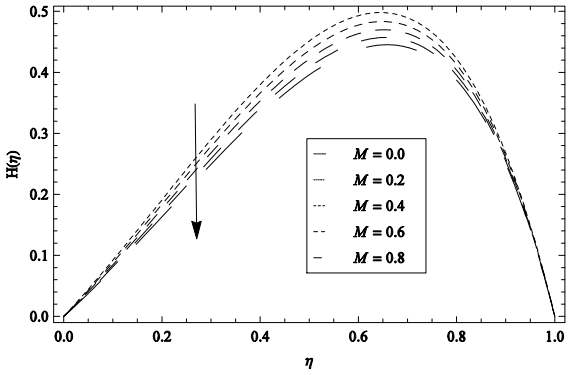
(e) For $R = 5$ and $\hbar = -0.5$



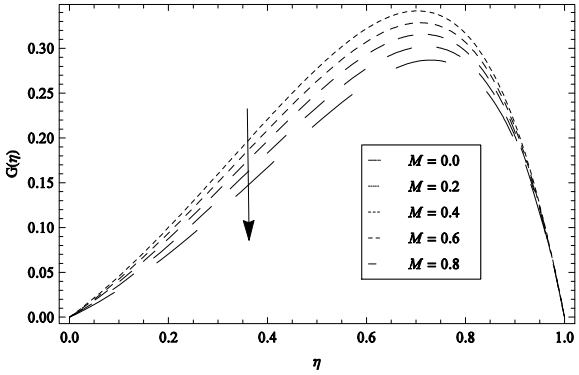
(f) For $R = 16$ and $\hbar = -0.27$

Fig. 3 Influence of stretching ratio γ for $M = 1$, $\lambda_1 = 2$, and $\lambda_2 = 2$ (a) w when $R = 5$, (b) w when $R = 16$, (c) u when $R = 5$, (d) u when $R = 16$, (e) P when $R = 5$, (d) P when $R = 16$.

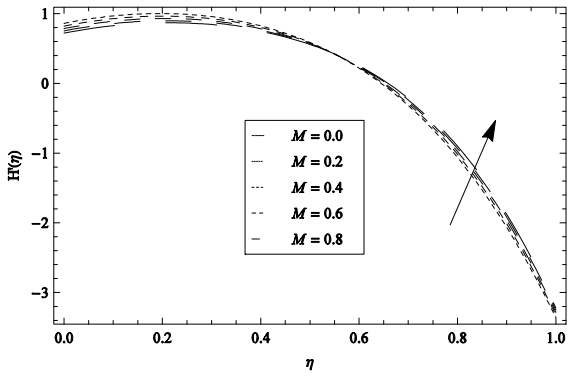
https://doi.org/10.1017/jmech.2015.25 Published online by Cambridge University Press



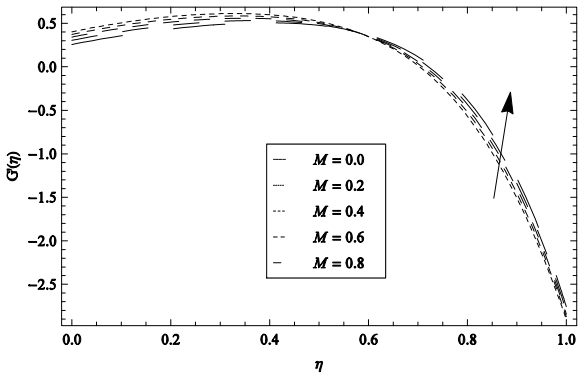
(a) For $R = 5$ and $\hbar = -0.5$



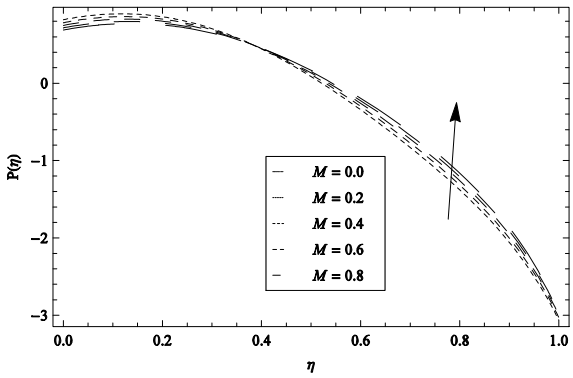
(b) For $R = 16$ and $\hbar = -0.27$



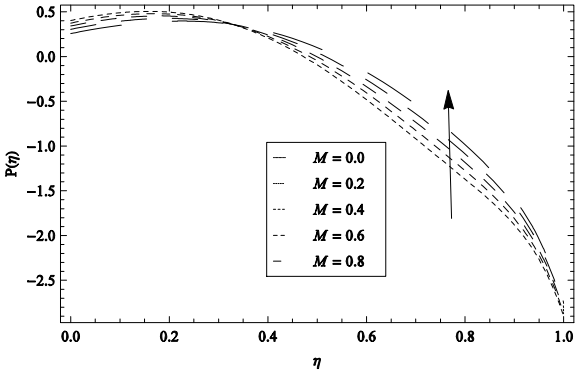
(c) For $R = 5$ and $\hbar = -0.5$



(d) For $R = 16$ and $\hbar = -0.27$



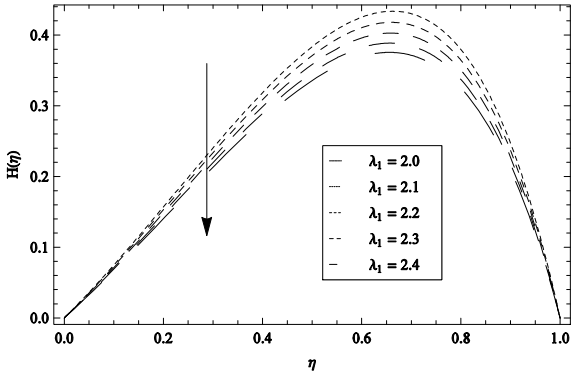
(e) For $R = 5$ and $\hbar = -0.5$



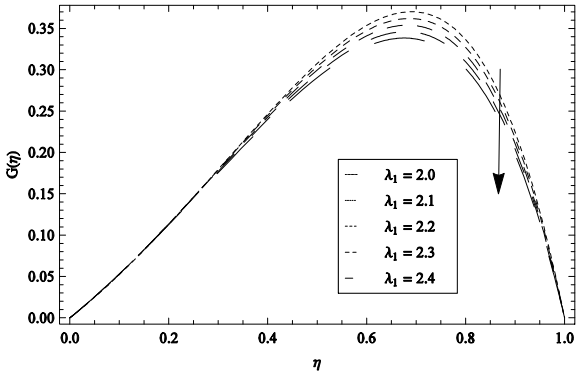
(f) For $R = 16$ and $\hbar = -0.27$

Fig. 4 Influence of Hartmann number M for $\gamma = 0.25$, $\lambda_1 = 2$, and $\lambda_2 = 2$ on (a) w when $R = 5$, (b) w when $R = 16$, (c) u when $R = 5$, (d) u when $R = 16$, (e) P when $R = 5$, (d) P when $R = 16$.

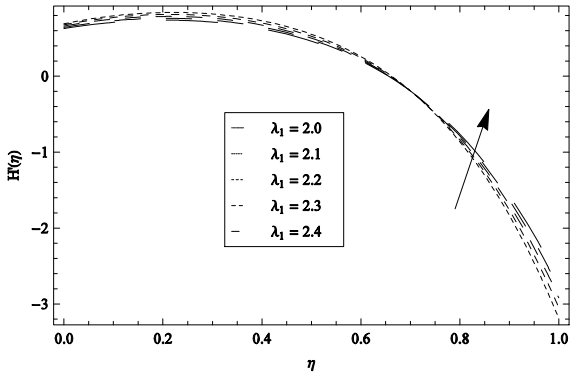
https://doi.org/10.1017/jmech.2015.25 Published online by Cambridge University Press



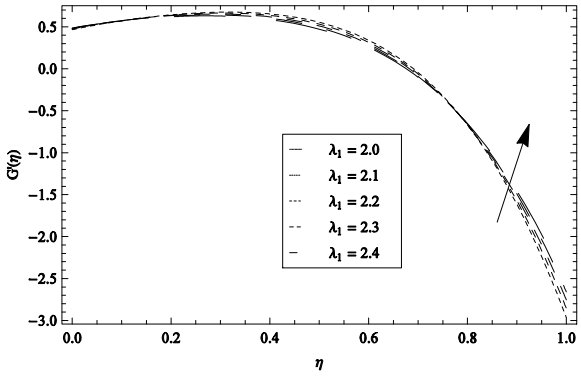
(a) For $R = 5$ and $\hbar = -0.5$



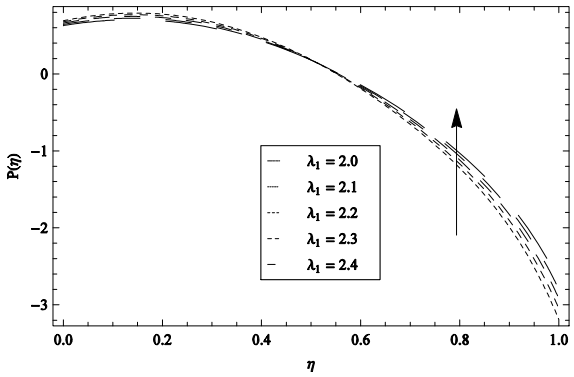
(b) For $R = 16$ and $\hbar = -0.27$



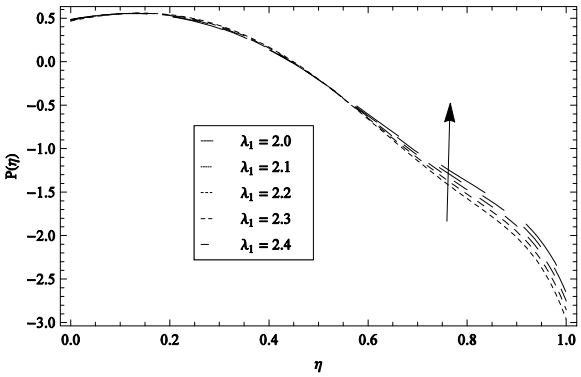
(c) For $R = 5$ and $\hbar = -0.5$



(d) For $R = 16$ and $\hbar = -0.27$



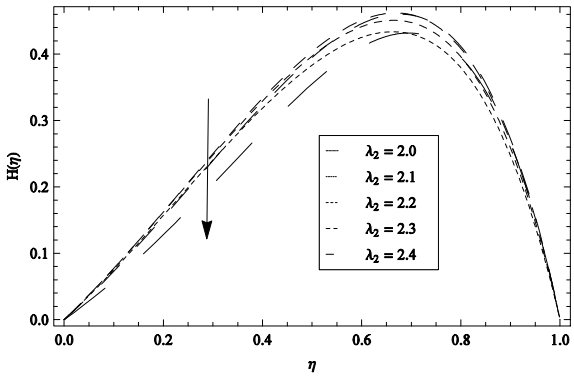
(e) For $R = 5$ and $\hbar = -0.5$



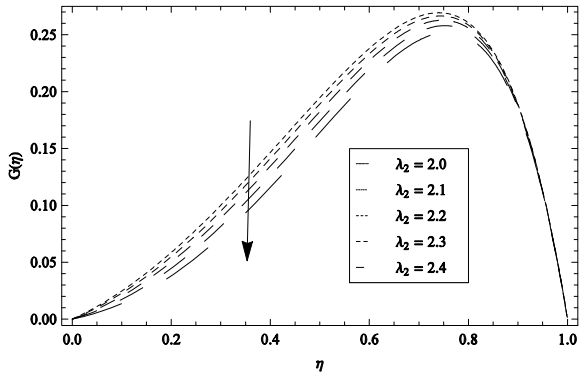
(f) For $R = 16$ and $\hbar = -0.27$

Fig. 5 Influence of slip parameter λ_1 for $\gamma = 0.25$, $M = 1$, $\lambda_2 = 2$ on (a) w when $R = 5$, (b) w when $R = 16$, (c) u when $R = 5$, (d) u when $R = 16$, (e) P when $R = 5$, (d) P when $R = 16$.

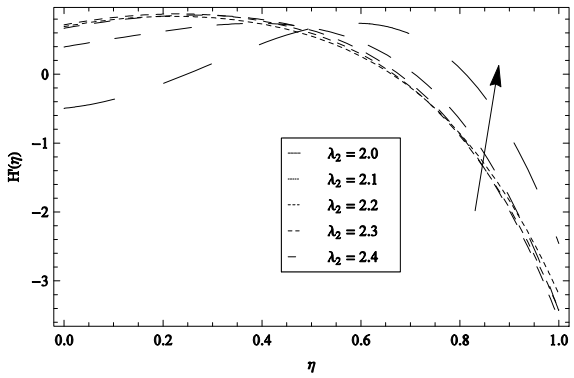
https://doi.org/10.1017/jmech.2015.25 Published online by Cambridge University Press



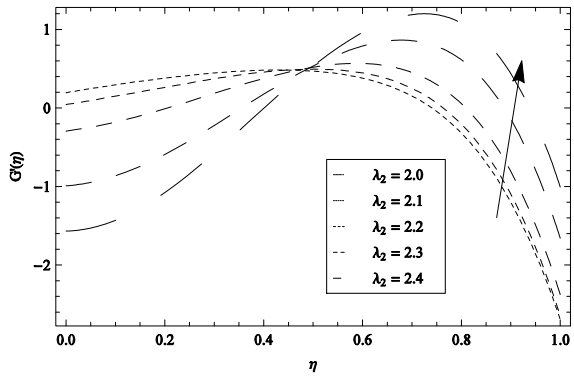
(a) For $R = 5$ and $\hbar = -0.5$



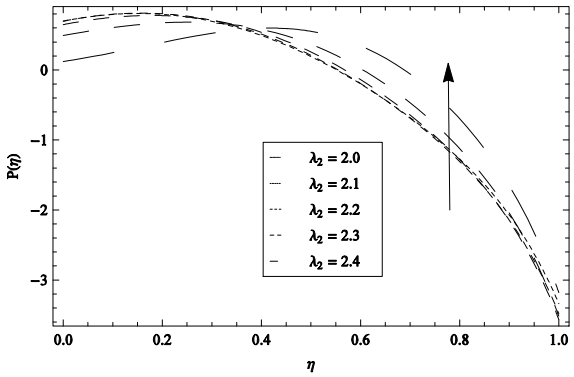
(b) For $R = 16$ and $\hbar = -0.27$



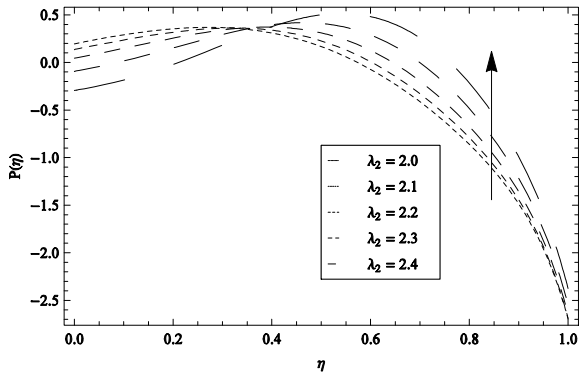
(c) For $R = 5$ and $\hbar = -0.5$



(d) For $R = 16$ and $\hbar = -0.27$



(e) For $R = 5$ and $\hbar = -0.5$



(f) For $R = 16$ and $\hbar = -0.27$

Fig. 6 Influence of slip parameter λ_2 for $\gamma = 0.25$, $M = 1$, $\lambda_1 = 2$ on (a) w when $R = 5$, (b) w when $R = 16$, (c) u when $R = 5$, (d) u when $R = 16$, (e) P when $R = 5$, (d) P when $R = 16$.

https://doi.org/10.1017/jmech.2015.25 Published online by Cambridge University Press

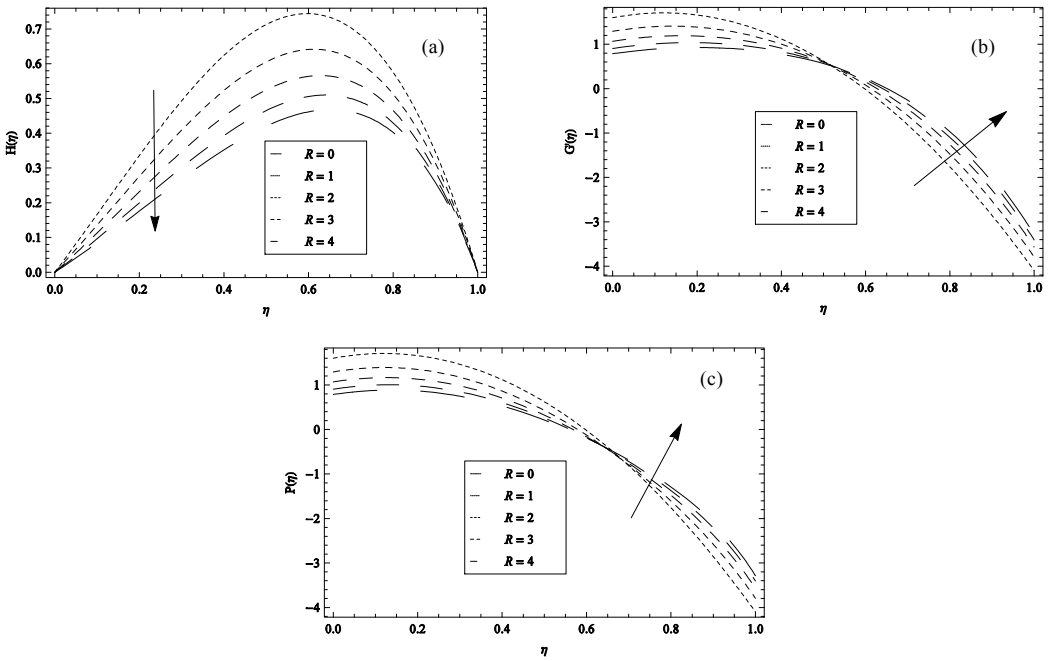


Fig. 7 Influence of Reynolds number R for $\gamma = 0.25$, $M = 1$, $\lambda_1 = 2$, and $\lambda_2 = 2$ on (a) z component of velocity w, (b) r component of velocity u, (c) pressure $P(\eta)$.

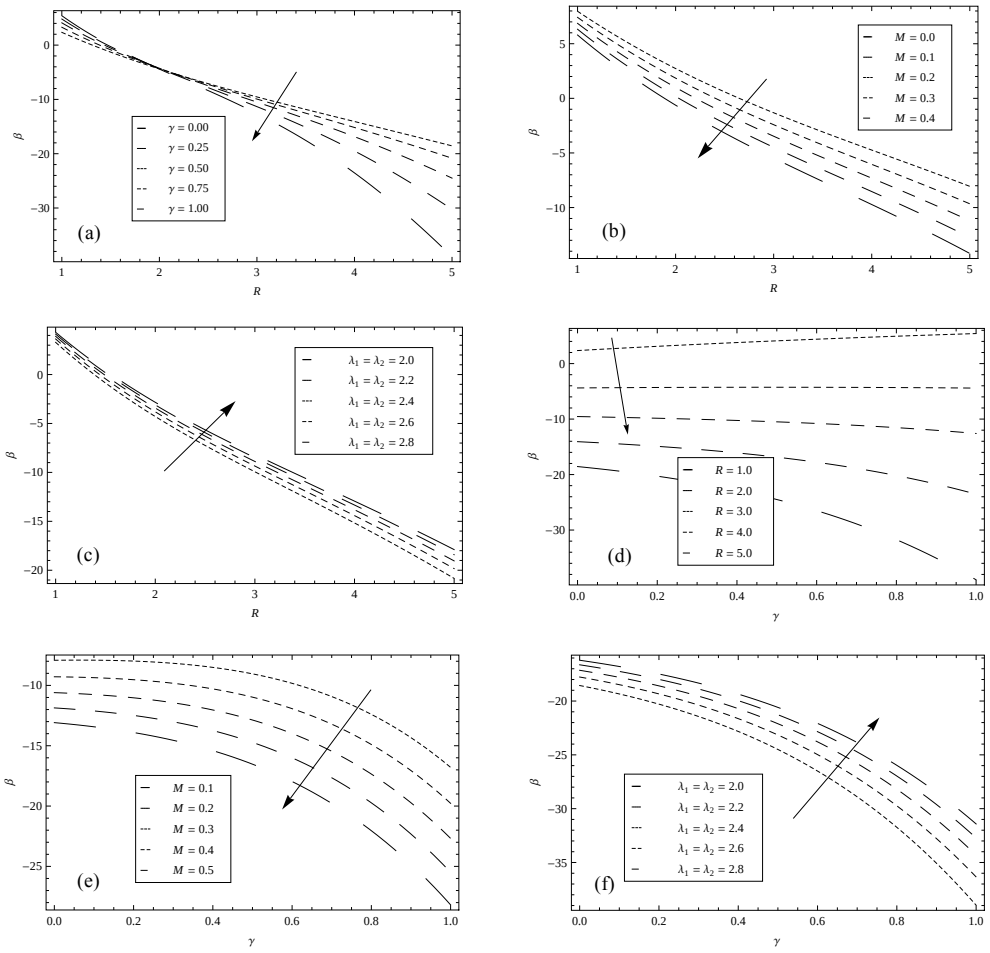


Fig. 8 The pressure parameter β: (a) ~ (c) represents β as a function of R, (a) $M = 1$, $\lambda_1 = 2$, $\lambda_2 = 2$, $\hbar = -0.5$, (b) for $\gamma = 0.25$, $\lambda_1 = 2$, $\lambda_2 = 2$, $\hbar = -0.5$, (c) for $\gamma = 0.25$, $M = 1$, $\hbar = -0.5$, (d) ~ (f) represents β as a function of γ, (d) for $M = 1$, $\lambda_1 = 2$, $\lambda_2 = 2$, $\hbar = -0.5$, (e) for $\lambda_1 = 2$, $\lambda_2 = 2$, $R = 5$, $\hbar = -0.5$, and (f) for $M = 1$, $R = 5$, $\hbar = -0.5$.

https://doi.org/10.1017/jmech.2015.25 Published online by Cambridge University Press

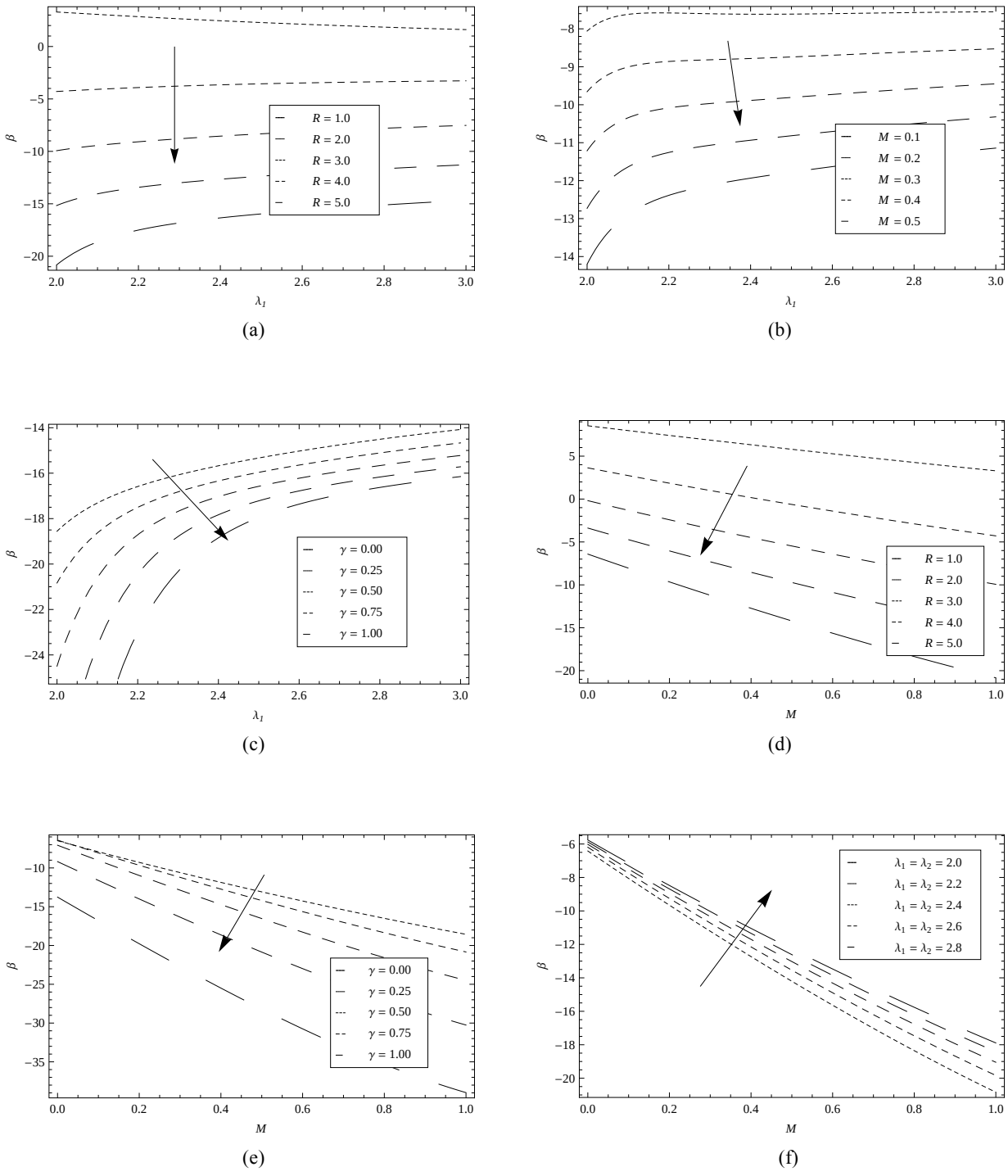
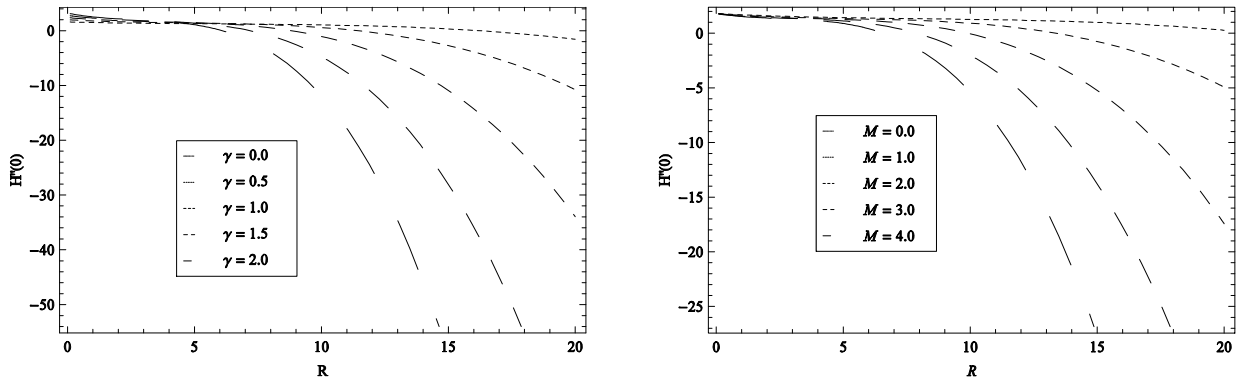


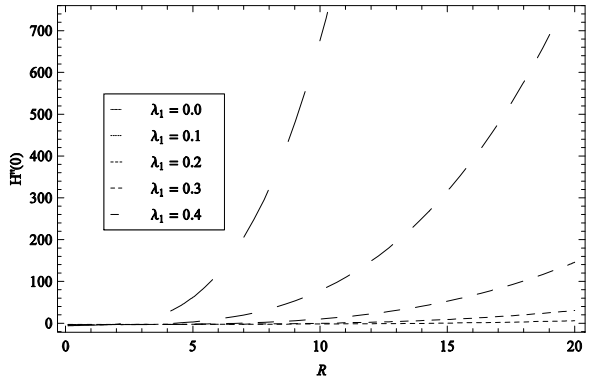
Fig. 9 The pressure parameter β: (a) ~ (c) represents β as a function of λ_1, (a) $\gamma = 0.25$, $M = 1$, $\lambda_2 = 2$, $\hbar = -0.5$, (b) for $\gamma = 0.25$, $M = 1$, $\lambda_2 = 2$, $\hbar = -0.5$, (c) for $M = 1$, $\hbar = -0.5$, $\lambda_2 = 2$, $R = 5$, (d) ~ (f) represents β as a function of γ, (d) for $\lambda_2 = 2$, $\lambda_1 = 2$, $\hbar = -0.5$, $\gamma = 0.25$, (e) for $\lambda_1 = 2$, $\lambda_2 = 2$, $R = 5$, $\hbar = -0.5$, and (f) for $M = 1$, $R = 5$, $\hbar = -0.5$.

https://doi.org/10.1017/jmech.2015.25 Published online by Cambridge University Press

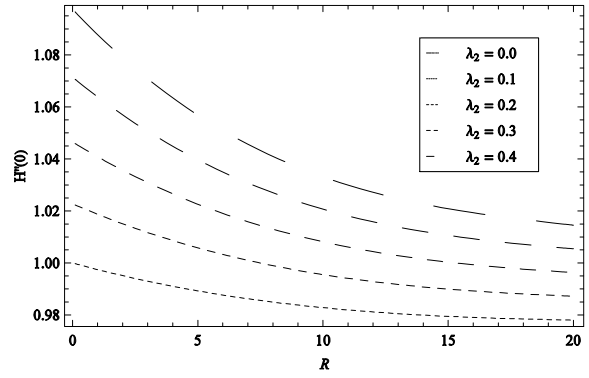


(a) Graph of C_{1f}

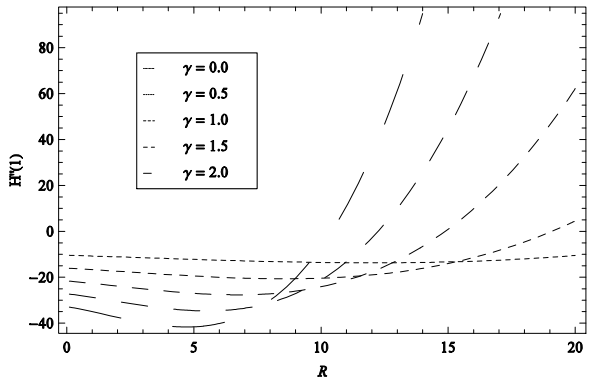
(b) Graph of C_{1f}



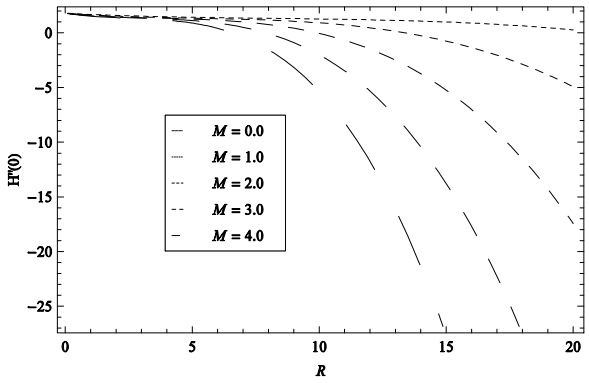
(c) Graph of C_{1f}



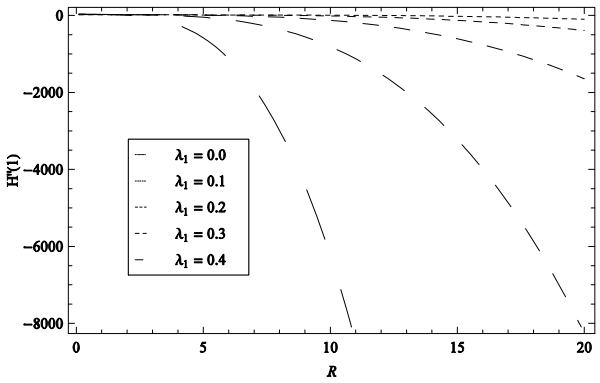
(d) Graph of C_{1f}



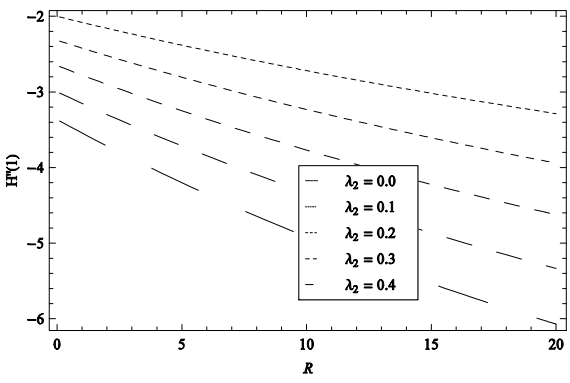
(e) Graph of C_{2f}



(f) Graph of C_{2f}



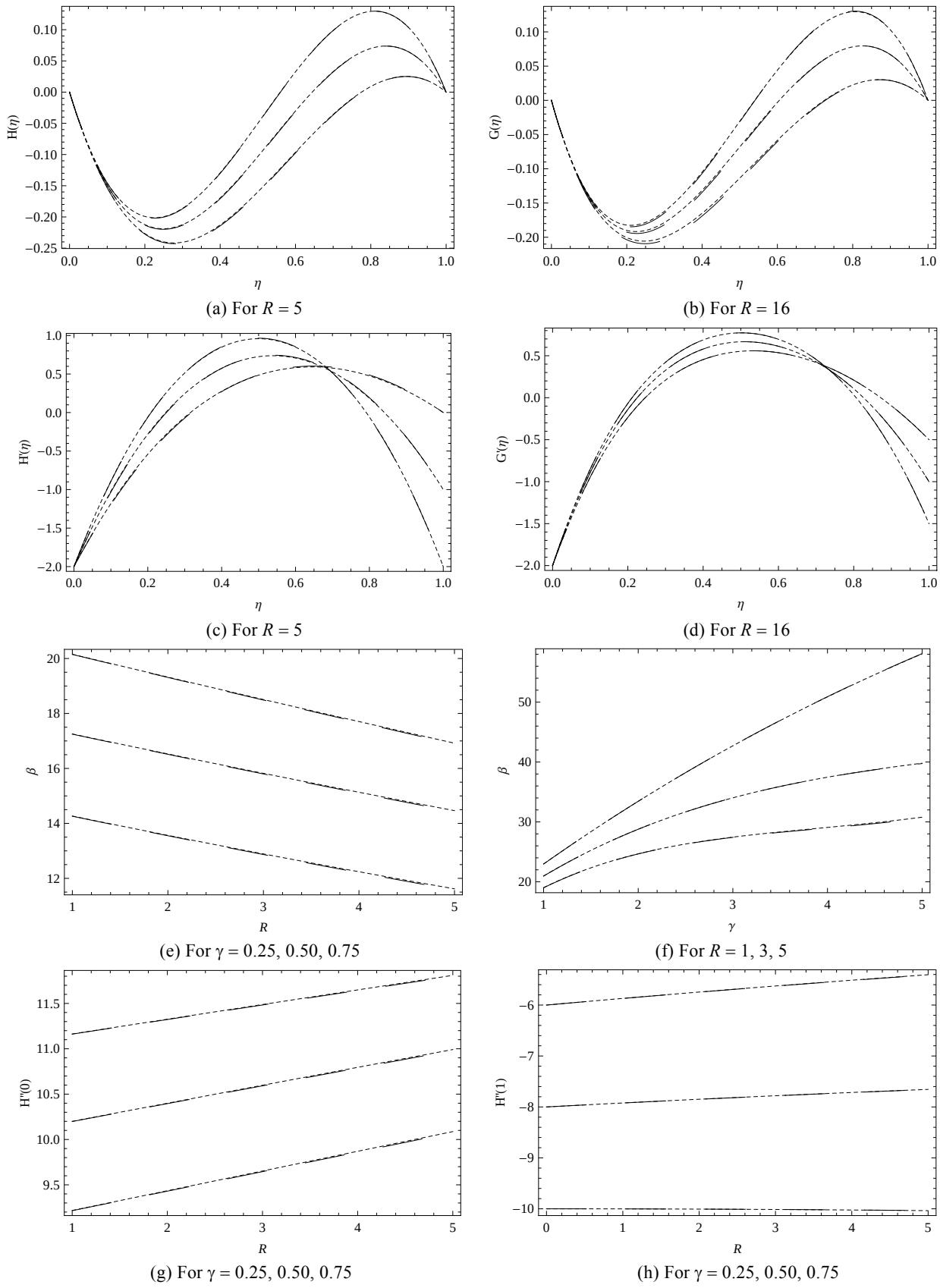
(g) Graph of C_{2f}



(h) Graph of C_{2f}

Fig. 10 The skin friction coefficient at lower disk as a function of Reynolds number for (a) for $M = 1$, $\lambda_1 = 2$, $\lambda_2 = 2$, $\hbar = -0.5$, (b) for $\gamma = 0.25$, $\lambda_1 = 2$, $\lambda_2 = 2$, $\hbar = -0.5$, (c) for $\gamma = 0.25$, $M = 1$, $\hbar = -0.5$, $\lambda_2 = 2$, (d) for $\gamma = 0.25$, $M = 1$, $\hbar = -0.5$, $\lambda_1 = 2$. The skin friction coefficient at upper disk as a function of Reynolds number for (e) for $M = 1$, $\lambda_1 = 2$, $\lambda_2 = 2$, $\hbar = -0.5$, (f) for $\gamma = 0.25$, $\lambda_1 = 2$, $\lambda_2 = 2$, $\hbar = -0.5$, (g) for $\gamma = 0.25$, $M = 1$, $\lambda_2 = 2$, $\hbar = -0.5$, (h) for $\gamma = 0.25$, $M = 1$, $\hbar = -0.5$, $\lambda_1 = 2$.

https://doi.org/10.1017/jmech.2015.25 Published online by Cambridge University Press



(a) For $R = 5$ (b) For $R = 16$

(c) For $R = 5$ (d) For $R = 16$

(e) For $\gamma = 0.25, 0.50, 0.75$ (f) For $R = 1, 3, 5$

(g) For $\gamma = 0.25, 0.50, 0.75$ (h) For $\gamma = 0.25, 0.50, 0.75$

Fig. 11 Comparison graphs, dash line represent present analytic solution and dotted line for solution of [15] in absence of magnetic field and slip: (a) ~ (d) represents the comparison of $H(\eta)$ for different value of $\gamma = 0.25$, 0.50, 0.75, (e) ~ (f) represent the comparison of β for different values γ and R respectively, (g) ~ (h) represent the comparison of $H''(0)$ and $H''(1)$ respectively.

https://doi.org/10.1017/jmech.2015.25 Published online by Cambridge University Press

6. CONCLUSIONS

Present paper investigates the axi-symmetry flow between two stretching disks in the presence of applied magnetic field and slip at the boundary. The obtained analytic solution through homotopy analysis method reveals following observations.

1. The Hartmann number decreases the z component of velocity and increases the γ component of velocity in the region where stretching ratio has significant effects.
2. By increasing the Hartmann number, pressure is found to increase in the region near the upper disk.
3. The slip at lower wall decreases velocity in the region near the lower disk. It also causes an increase in radial component of velocity in region near the upper disk.
4. Qualitatively, the behavior of slip at upper disk is opposite to that of slip at lower disk.
5. In the region near the lower disk, the pressure is decreasing function of slip parameter λ_1. while in the region near the upper disk, pressure increasing as λ_1 increases.
6. The influence of slip at upper disk on velocity components and pressure is opposite to that of slip at lower disk.
7. It is seen that the shear stresses on the surfaces of disk decreases with the increase of stretching ratio, Hartmann number and increases with the increases of slip parameter λ_1 and λ_2.

FINANCIAL SUPPORT

This work is supported by the Indigenous Ph.D. Scholarship Scheme of Higher Education Commission (HEC) Pakistan.

REFERENCES

1. Altan, T., Oh, S. and Gegel, H., *Metal Forming Fundamentals and Applications*, American Society of Metals, Metals Park, OH (1979).
2. Fisher, E. G., *Extrusion of Plastics*, Wiley, New York (1976).
3. Tadmor, Z. and Klein, I., *Engineering Principles of Plasticating Extrusion*, *Polymer Science and Engineering Series*, Van Norstrand Reinhold Co., New York (1970).
4. Sakiadis, B. C., "Boundary-Layer Behavior on Continuous Solid Surface: I. Boundary-Layer Equations for Two-Dimensional and Axi-Symmetric Flow," *AIChE Journal*, pp. 26–28 (1961).
5. Sakiadis, B. C., "Boundary-Layer Behavior on Continuous Solid Surface: II. Boundary-Layer on Continuous Flat Surface," *AIChE Journal*, pp. 221–225 (1961).
6. Crane, L. J., "Flow Past a Stretching Plate," *Zeitschrift für angewandte Mathematik Und Physik*., (ZAMP), **21**, pp. 645–647 (1970).
7. Gupta, P. S. and Gupta, A. S., "Heat and Mass Transfer on a Stretching Sheet with Suction and Blowing," *The Canadian Journal of Chemical Engineering*, **58**, pp. 744–746 (1977).
8. Brady, J. F. and Acrivos, A., "Steady Flow in a Channel or Tube with Accelerating Surface Velocity. An Exact Solution to the Navier-Stokes Equations with Reverse Flow," *Journal of Fluid Mechanics*, **112**, pp. 127–150 (1981).
9. McLeod, J. B. and Rajagopal, K. R., "On the Uniqueness of Flow of a Navier-Stokes Fluid Due to a Stretching Boundary," *Archive for Rational Mechanics and Analysis*, **98**, pp. 385–393 (1987).
10. Wang, C. Y., "The Three Dimensional Flow Due to a Stretching Flat Surface," *Physics of Fluids*., **27**, pp. 1915–1917 (1984).
11. Wang, C. Y., "Fluid Flow Due to a Stretching Cylinder," *Physics of Fluids*, **31**, pp. 466–468 (1988).
12. Mahapatra, T. R. and Gupta, A. S., "Heat Transfer in Stagnation-Point Flow Towards a Stretching Surface," *Heat and Mass Transfer*, **38**, pp. 517–521 (2002).
13. Fang, T., "Flow over a Stretchable Disk," *Physics of Fluids*, **19**, p. 128105 (2007).
14. Fang, T. and Zhang, J., "Flow Between Two Stretchable Disks—An Exact Solution of the Navier-Stokes Equations," *International Communication in Heat and Mass Transfer*, **35**, pp. 892–895 (2008).
15. Gorder, R. A. V., Sweet, E. and Vajravelu, K., "Analytical Solutions of a Coupled Nonlinear System Arising in a Flow Between Stretching Disks," *Applied Mathematics and Computations*, **216**, pp. 1513–1523 (2010).
16. Wang, C. Y., "Flow Due to a Stretching Boundary with Partial Slip-An Exact Solution of the Navier-Stokes Equations," *Chemical Engineering Science*, **57**, pp. 3745–3747 (2002).
17. Anderson, H. I., "Slip Flow Past a Stretching Surface," *Acta Mechanica*, **158**, pp. 121–125 (2002).
18. Ariel, P. D., "Axisymmetric Flow Due to a Stretching Sheet with Partial Slip," *Computers and Mathematics with Applications*, **54**, pp. 1169–1183 (2007).
19. Sajid, M., Ahmad, I. and Hayat, T., "Unsteady Boundary Layer Flow Due to a Stretching Sheet in Porous Medium with Partial Slip," *Journal of Porous Media*, **12**, pp. 911–917 (2009).
20. Sajid, M., Ali, N., Abbas, Z. and Javed, T., "Stretching Flows with General Slip Boundary Condition," *International Journal of Modern Physics B*, **30**, pp. 5939–5947 (2010).
21. Davidson, P. A., *An Introduction to Magnetohydrodynamics*, Cambridge University Press, Cambridge (2001).
22. Hayat, T., Shafiq, A., Nawaz, M. and Alsaedi, A., "MHD Axisymmetric Flow of Third Grade Fluid Between Porous Disks with Heat Transfer," *Applied Mathematics and Mechanics (English Edition)*, **33**, pp. 749–764 (2012).

https://doi.org/10.1017/jmech.2015.25 Published online by Cambridge University Press

23. Hayat, T., Naz, R. and Sajid, M., "On the Homotopy Solution for Poiseuille Flow of a Fourth Grade Fluid," *Communication in Nonlinear Science and Numerical Simulation*, **15**, pp. 581–589 (2010).
24. Sajid, M., Awaisb, M., Nadeemb, S. and Hayat, T., "The Influence of Slip Condition on Thin Film Flow of a Fourth Grade Fluid by the Homotopy Analysis Method," *Computers Mathematics with Applications*, **56**, pp. 2019–2026 (2008).
25. Sajid, M. and Hayat, T., "The Application of Homotopy Analysis Method to Thin Film Flows of a Third Order Fluid," *Chaos Solitons and Fractals*, **38**, pp. 506–515 (2008).
26. Sajid, M. and Hayat, T., "The Application of Homotopy Analysis Method for MHD Viscous Flow Due to a Shrinking Sheet," *Chaos Solitons and Fractals*, **39**, pp. 1317–1323 (2009).
27. Sajid, M., Abbas, Z. and Hayat, T., "Homotopy Analysis for Boundary Layer Flow of a Micropolar Fluid Through a Porous Channel," *Applied Mathematical Modelling*, **33**, pp. 4120–4125 (2009).
28. Sajid, M., Siddiqui, A. and Hayat, T., "Wire Coating Analysis Using MHD Oldroyd 8-Constant Fluid," *International Journal of Engineering Sciences*, **45**, pp. 381–392 (2007).
29. Sajid, M., Hayat, T. and Asghar, S., "Non-Similar Analytic Solution for MHD Flow and Heat Transfer in a Third-Order Fluid over a Stretching Sheet," *International Journal of Heat and Mass Transfer*, **50**, pp. 1723–1736 (2007).
30. Sajid, M., Hayat, T. and Asghar, S., "Non-Similar Solution for the Axisymmetric Flow of a Third-Grade Fluid over Radially Stretching Sheet," *Acta Mechanica*, **189**, pp. 193–205 (2007).
31. Liao, S. J., *Beyond Perturbation: Introduction to the Homotopy Analysis Method*, Chapman and Hall, Boca Raton (2003).
32. Liao, S. J., "On the Analytic Solution of Magnetohydrodynamic Flow of Non-Newtonian Fluids over a Stretching Sheet," *Journal of Fluid Mechanics*, **488**, pp. 189–212 (2003).
33. Liao, S. J., "Notes on Homotopy Analysis Method: Some Definitions and Theorems," *Communications in Nonlinear Science and Numerical Simulation*, **14**, pp. 983–997 (2009).
34. Liao, S. J., "An Optimal Homotopy Analysis Approach for Strongly Nonlinear Differential Equations," *Communications in Nonlinear Science and Numerical Simulation*, **15**, pp. 2003–2016 (2010).

(Manuscript received July 19, 2014,
accepted for publication December 14, 2014.)

https://doi.org/10.1017/jmech.2015.25 Published online by Cambridge University Press